Eutrophication-driven *Trichodesmium erythraeum* blooms in Karimunjawa National Park, Indonesia

Original Article

LIMNOLOGY FRESHWATER BIOLOGY

Widiaratih R.[1,2*], Patil C.Ya.[2], Wirasatriya A.[1], Putranto A.B.[3], Maslukah L.[1], Widianingsih[4], Pranowo W.S.[5], Himawan D.[1], Satya E.D.[6]

[1] *Department of Oceanography, Faculty of Marine and Fishery, University of Diponegoro, Jl. Prof. Jacob Rois, Central Java, 50275, Indonesia*
[2] *Department of Naval Architecture, Ocean & Marine Engineering, University of Strathclyde, 16 Richmond Street, Glasgow, G1 1XQ, United Kingdom*
[3] *Department of Industrial Technology, Vocational School Universitas Diponegoro, Jl. Prof. Jacob Rois, Tembalang, Semarang, Central Java, 50275, Indonesia*
[4] *Department of Marine Science, Faculty of Marine and Fishery, Faculty of Marine and Fishery, University of Diponegoro, Jl. Prof. Jacob Rois, Central Java, 50275, Indonesia*
[5] *Research Center for Climate and Atmosphere (PRIMA), National Research and Innovation Agency, Jl. Djunjunan No. 133, Bandung, 40174, Indonesia*
[6] *Director of Water and Air Police (Ditpolairud), Regional Police of Central Java, Jl. Yos Sudarso, No. 57, Semarang, Central Java, 50174, Indonesia*

ABSTRACT. Harmful algal blooms (HABs) are increasingly frequent due to anthropogenic nutrient enrichment, posing significant ecological and economic threats. It includes hypoxia, toxin production, and a decline in tourism due to odour pollution. This study investigates the HAB event in Karimunjawa National Park (KNP) on September 19, 2023, attributed to nutrient loading from inadequate wastewater treatment in the shrimp pond. The bloom coincided with the shrimp harvest season, indicating a strong correlation between pond effluents and coastal eutrophication. To identify the dominant algal species and primary environmental drivers of bloom formation, nutrients and water quality parameters were analysed using field and satellite observations from three locations in KNP. Pearson's correlation analysis was applied to assess linear relationships among variables, while principal component analysis (PCA) was employed to determine key contributors to HAB development. The findings indicate that *Trichodesmium erythraeum* was the dominant bloom-forming species, proliferating due to biogeochemical imbalances induced by excessive nutrient enrichment. Phosphate ($r = 0.952$), silicate ($r = 0.832$), ammonia ($r = 0.670$), and nitrate ($r = 0.653$) were identified as key factors influencing bloom dynamics. Lower ammonia concentrations suggest uptake by phytoplankton, whereas microbial decomposition contributed to elevated phosphate levels. Additionally, high sunlight exposure ($r = 0.877$) and low-currents hydrodynamic conditions ($r = 0.197$) further facilitated bloom persistence. These findings underscore the urgent need for enhanced wastewater management policies in shrimp ponds and stricter environmental policies to mitigate future HABs occurrences and protect marine ecosystems and coastal economies.

Keywords: wastewater treatment, eutrophication, HAB, sunlight, hydrodynamics, biogeochemical cycle

For citation: Widiaratih R., Patil C.Ya., Wirasatriya A., Putranto A.B., Maslukah L., Widianingsih, Pranowo W.S., Himawan D., Satya E.D. Eutrophication-driven *Trichodesmium erythraeum* blooms in Karimunjawa National Park, Indonesia // Limnology and Freshwater Biology. 2025. - № 6. - P. 1268-1280. DOI: 10.31951/2658-3518-2025-A-6-1268

1. Introduction

The increase in harmful algal blooms (HABs) due to anthropogenic (human-driven) factors has become a major environmental concern. Key drivers include agricultural runoff (fertilizers), sewage discharge, industrial waste, and urban stormwater, all of which contribute excess nutrients to coastal waters and promote algal overgrowth. Recently, the HAB event had been documented in Karimunjawa National Park (KNP), Indonesia, highlighting that even marine protected areas are not immune to the pressures of human-induced nutrient pollution and environmental change.

KNP is a marine conservation area of high ecological significance, supporting diverse coral reefs, reef fish, mangroves, and seagrass beds. These ecosystems contribute to coastal resilience, biodiversity conservation, and fisheries sustainability (Yuliana et al., 2017; Wijayanti et al., 2018;). The park's pristine marine

*Corresponding author. E-mail address: rikha.widiaratih@live.undip.ac.id (R. Widiaratih)

Received: July 18, 2025;
Accepted after revised: November 07, 2025;
Available online: December 25, 2025

environment attracts domestic and international tourists, with activities such as snorkelling, diving, and cultural tourism driving a growing ecotourism industry (Satya et al., 2023). This sector has become a key economic driver, providing employment and supporting local livelihoods (Wijaya et al., 2021).

The KNP community has expanded into the Vannamei shrimp (*Litopenaeus vannamei*) pond, a key Indonesian fishery export commodity (Sidqi et al., 2022). However, its rapid expansion within KNP lacks adequate wastewater treatment, leading to unregulated effluent discharge and coastal water degradation due to insufficient regulatory oversight (Purnomo et al., 2022). Excessive nutrient enrichment from shrimp farming had contributed to HAB characterized by uncontrolled algal proliferation and toxin production, posing risks to marine biodiversity, human health, and coastal ecosystems (Endean et al., 1993).

The local community expressed significant concern over the HAB outbreak in KNP on September 19, 2023, following noticeable seawater discoloration (green, red, and black hues) and a strong unpleasant odour. These phenomena were reported in several coastal areas, particularly near shrimp ponds and popular beach locations, including Bobby Beach, Legon Lele Beach, and Menjangan Besar Island (Fig. 1). Recognizing the potential negative impact on tourism, residents initiated remedial actions to restore beach conditions. On September 22, 2023, a cleanup initiative was undertaken, involving seawater extraction using pumps to mitigate the effects of HAB.

HAB has detrimental impacts on the aquatic ecosystem of KNP. One notable consequence of HAB was the fish mortality in fishponds near Menjangan Besar Island, attributed to elevated nutrient levels from shrimp pond effluents, which contain excess shrimp feed residues and metabolic waste. These nutrient-rich conditions, coupled with optimal sunlight exposure, facilitated algal proliferation, leading to a sharp increase in dissolved oxygen (DO) consumption by algae. As a result, DO levels dropped below seawater quality standards, causing hypoxia-induced fish mortality (Boyd et al., 1975). Beyond direct fish mortality, HABs also contribute to seafood contamination, particularly in fish and shellfish, posing serious public health risks. Contaminated seafood may contain toxins responsible for amnesic, diarrhetic, azaspiracid, neurotoxic, and paralytic shellfish poisoning (Morabito et al., 2018). Following the HAB events, the subsequent algal decomposition process further exacerbates marine ecosystem degradation. Decomposing algae settle on the seabed, leading to sedimentation, which obstructs sunlight penetration and increases organic matter accumulation. This triggers microbial activity, resulting in oxygen depletion, reduced pH levels, and coral tissue degradation, ultimately threatening coral reef sustainability (Weber et al., 2012).

HAB can be quantified using Chlorophyll-a (Chl-a) concentrations, a key indicator of phytoplankton biomass (Wang et al., 2017) and water fertility (Doering et al., 2006). HAB formation is typically driven by nutrient enrichment (ammonia, phosphate, nitrate, and silicate) (Paerl et al., 2007), water quality variables (total suspended solids (TSS), temperature, dissolved oxygen (DO), salinity, and pH) (Harvey et al., 2019), and hydrodynamic factors (currents, waves, and tides) (Qijun, 2010). However, the complex interactions between these factors and HAB dynamics remain poorly understood. This study aimed to explore the causes of HAB in KNP by identifying the main algal species involved and their links to nutrient input from shrimp ponds, water quality, and ocean currents.

Understanding the dominant algal species and the key environmental drivers of bloom formation is essential for predicting and managing HABs. Since different species vary in toxicity and ecological impact, identifying them improves risk assessment and response strategies. Environmental factors such as nutrient loading, temperature, and salinity, along with water quality indicators like TSS, DO, and pH, offer a critical insight into bloom dynamics. Together, these variables support improving the understanding of HAB dynamics and

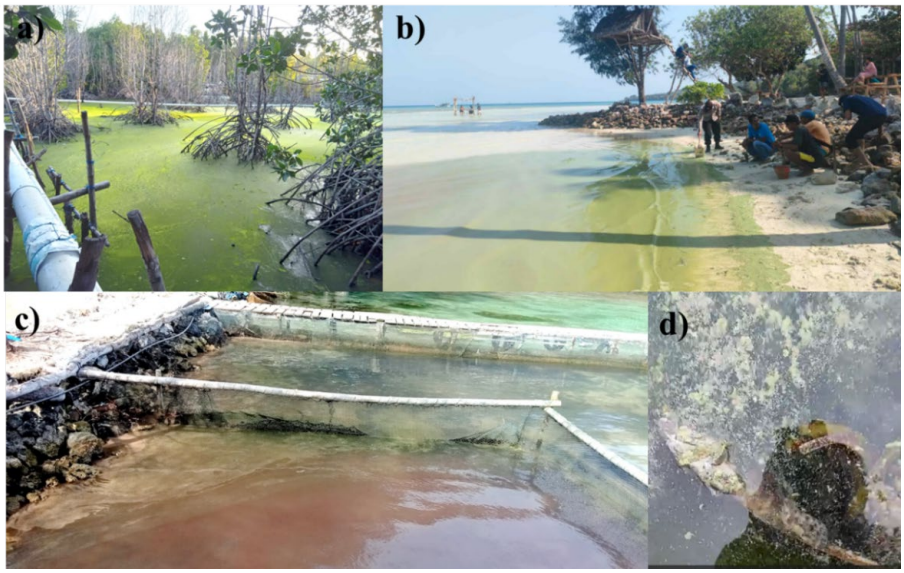

Fig.1. HABs in Karimunjawa, September 19, 2023 at: a) Mangrove area near fishpond; b) Bobby Beach; c) Menjangan Besar Island; and d) fish mortality in fish pond near Menjangan Besar Island.

guide effective water quality management. The objectives of this study were to: (i) identify bloom-forming algal and measure microalgae abundance; (ii) assess quantitatively distribution value of Chl-a, nutrients, TSS, water quality, and current patterns during and after the bloom, and (iii) examine the relationships between these factors. The results offer new insights into the HAB development and its environmental drivers in KNP.

2. Materials and Methods

2.1. Materials

KNP comprises 27 islands, with Karimunjawa Island being the largest and most densely populated. However, Vannamei shrimp farming has expanded rapidly, with the plot of 33 shrimp ponds identified along Karimunjawa Island's coastline by 2022 (Fig. 2), raising concerns about coastal environmental impacts. This study utilizes field data (Table 1) and satellite data (Table 2).

HAB and their interactions with Chl-a, TSS, and nutrients are strongly influenced by seawater quality and ocean surface currents. Due to the limited availability of field data, seawater parameters (sea surface temperature, DO, salinity, and pH) and surface currents on September 19 and 22, 2023, were obtained from satellite and numerical model sources (Table 2). While satellite data provides high temporal resolution, its spatial limitations, particularly in coastal areas, necessitate interpolation, which may reduce accuracy (Apostolopoulos et al., 2020). Despite these constraints, satellite-derived data enables the identification of spatiotemporal patterns during and after HABs cleanup, offering a comprehensive assessment of environmental dynamics.

During the field visit to Karimunjawa National Park (KNP) on September 22, 2023, the authors encountered a special situation: HABs had already been cleaned up by the local community to reduce impacts on marine tourism. As a result, direct sampling of the HABs was not possible at that time. However, samples from the most severely affected areas characterized by red-coloured seawater around Menjangan Besar Island and green-coloured seawater at Bobby Beach were obtained from local community members, who had collected surface water samples during the bloom event (September 19, 2023). These samples are indicated with red circles in Fig. 2. Consequently, the available HAB-related samples are limited in both spatial and temporal coverage. Nevertheless, these few samples provide valuable insight into the severity of the HAB event, even after the clean-up.

Post-cleanup surface water samples (2L each) were collected on September 22, 2023, from the shrimp pond outlet, Legon Lele Beach, Bobby Beach, and Menjangan Besar Island. At the shrimp pond outlet, a single sample was taken, while at the other sites, three samples were collected from different zones, including the shoreline, the mid-zone, and the furthest accessible point (indicated with green circles in Fig. 2). All surface water samples (2L each) were analysed for Chl-a, TSS, and nutrient concentrations, including ammonia, silicate, phosphate, and nitrate, under two conditions such as during the HAB event (September 19, 2023) and after the clean-up (September 22, 2023) (Table 1).

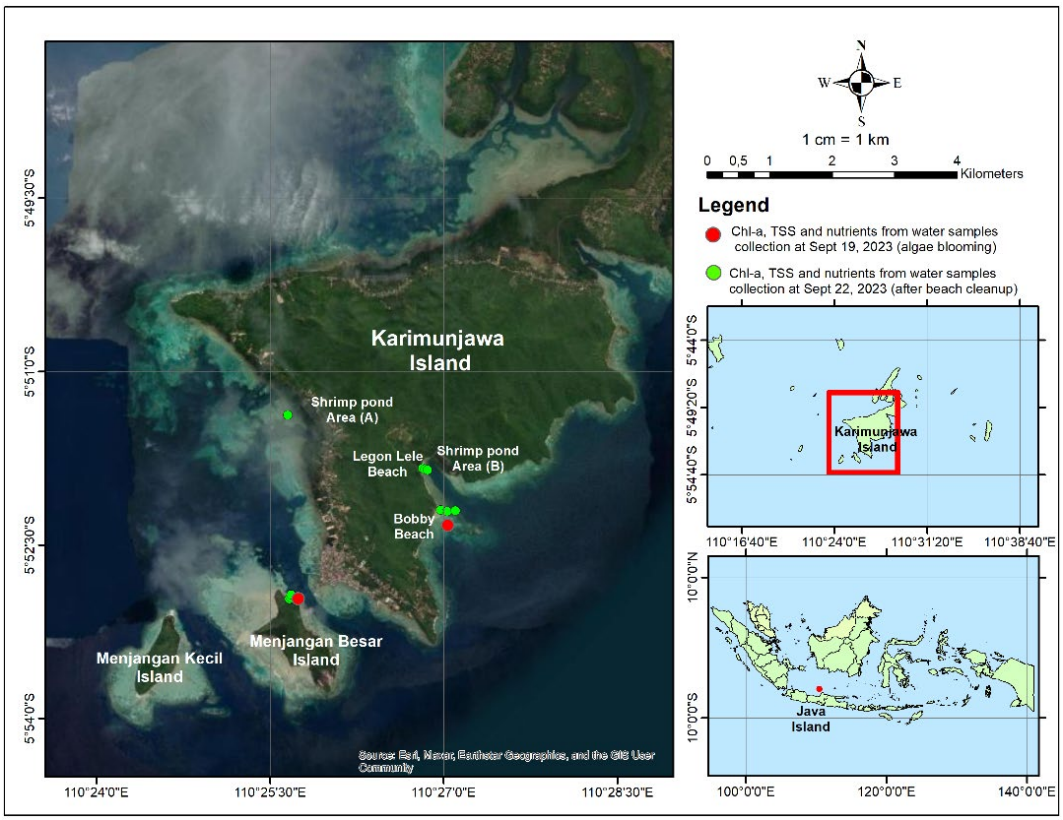

Fig.2. Reseach Area.

Table 1. Data source of field observation for Chl-a, TSS, and nutrients

Data	Samples	Date	Method
Chl-a	Surface water samples of 2 Liters for each station	1. During algal blooming on September 19, 2023, in Bobby beach and Menjangan Besar Island 2. After algal blooming cleanup on September 22, 2023, in Bobby Beach (3 stations), Legon Lele Beach (3 stations), Menjangan Besar Island (3 stations), shrimp pound channel (1 station)	APHA, 2005
Total Suspended Solid (TSS)			Chan et al., 2008
Ammonia			Zadorojny and Saxton, 1973; Parsons et al., 1984
Silicate			Mullin and Riley, 1955; Parsons et al., 1984
Phosphate			Murphy and Rilley, 1962; Parsons et al., 1984
Nitrate			Morris and Riley, 1963; Parsons et al., 1984

2.2. Methods

Surface water samples were analysed in the laboratory following standardized protocols. Samples were stored in sealed bottles within a cool, dark environment to prevent degradation. Processing methods for Chl-a, TSS, and nutrients are detailed in Table 1. Chl-a was analysed via APHA spectrometry (Johan et al., 2014), while TSS was determined by measuring suspended solids in 1 L of filtered water (Chan et al., 2008). Nutrients were analysed using established method including ammonia (Parsons et al., 1984; Zadorojny and Saxton, 1973), nitrate (Morris and Riley, 1963; Parsons et al., 1984), phosphate (Murphy and Rilley, 1962; Parsons et al., 1984), and silicate (Mullin and Riley, 1955; Parsons et al., 1984). Algal species were identified using binocular microscopy (400 × magnification) (Lessard and Swift, 1986; Veldhuis and Kraay, 2000), and microalgae abundance was calculated using Stirling's formula (Stirling, 1999):

$$N = \frac{nxv}{V} \quad (1),$$

where N – total phytoplankton cells per Liter, n – average phytoplankton cells in 1 mL of sample, v – volume of plankton concentrates (mL), and V – volume of water filtered (L). The result is expressed as cells per Liter (cells/L).

This study aims to identify key parameters influencing the HAB occurrence, focusing on nutrients, TSS, and water quality. Statistical analysis was conducted using Pearson's correlation and principal component analysis (PCA) to examine intervariable relationships. Pearson's correlation quantifies linear relationships between two variables (Liu, 2019), while PCA extends this approach to identify patterns among multiple variables. The Pearson correlation matrix is particularly useful in PCA when variables have different scales or units, necessitating standardization to ensure equal contributions. This allows PCA to emphasize relationships rather than absolute values (Polak et al., 2009). PCA offers several advantages, including dimensionality reduction, which condenses complex datasets while preserving key variance, facilitating clearer pattern identification. Additionally, PCA also provides dimensionality reduction, mitigates multicollinearity, and enhances data visualization, making it a powerful tool for analysing complex environmental interactions such as HAB formation (Patel et al., 2024).

Table 2. Data on water quality (SST, pH, Salinity, and DO) and hydrodynamics (currents) from satellite data

Data	Source	Spatial resolution	Temporal resolution	Access date	Website
Sea surface temperature	Operational Sea Surface Temperature and Ice Analysis (OSTIA)	0.05° × 0.05°	Daily	Dec 20, 2024	https://data.marine.copernicus.eu/product/SST_GLO_SST_L4_NRT_OBSERVATIONS_010_001/description
pH	Numerical model results	0.25° × 0.25°	Daily	Dec 20, 2024	https://data.marine.copernicus.eu/product/GLOBAL_ANALYSISFORECAST_BGC_001_028/description
Salinity	NASA's Soil Moisture Active Passive (SMAP) dan ESA's Soil Moisture Ocean Salinity (SMOS)	0.125° × 0.125°	Daily	Dec 20, 2024	https://data.marine.copernicus.eu/product/MULTIOBS_GLO_PHY_S_SURFACE_MYNRT_015_013/description
Dissolved oxygen (DO)	Numerical model results	0.25° × 0.25°	Daily	Dec 20, 2024	https://data.marine.copernicus.eu/product/GLOBAL_ANALYSISFORECAST_BGC_001_028/description
Sea surface currents	Numerical model (The Operational Mercator global ocean analysis and forecast)	0.083° × 0.083°	Daily	Dec 28, 2024	https://data.marine.copernicus.eu/product/GLOBAL_ANALYSISFORECAST_PHY_001_024/description

3. Results and discussion

3.1. Type and abundance of algal species HAB in KNP, Indonesia

Microalgal species identification was conducted through binocular microscopy at two locations at Bobby Beach and Menjangan Besar Island. Observations based on taxonomic classification (Guiry and Guiry, 2023) confirmed that *Trichodesmium erythraeum* Ehrenberg ex Gomont, 1892 was the bloom-forming species. *Trichodesmium erythraeum* is classified within the phylum Cyanophyta (Cyanobacteria) due to its peptidoglycan-containing cell walls (Fraga et al., 2025). As a prokaryotic organism, it lacks a true nucleus and forms filamentous colonies (Fig. 3). Instead of a nucleus, it contains a pseudo-nucleus with thylakoids, which play a crucial role in light absorption through specialized pigments called phycobilin (Frankenberg et al., 2001).

Trichodesmium erythraeum is a filamentous, diazotrophic cyanobacterium that fixes nitrogen in oligotrophic, subtropical, and tropical oceans, including Indonesian waters, sustaining marine productivity (Ding et al., 2022). Its blooms, driven by warm temperatures, nutrient inputs, and climate variability, shift from green (phycocyanin and allophycocyanin) in early stages to red (phycoerythrin and carotenoids) during senescence, releasing nutrients and potentially contributing to oxygen depletion and toxin production (Coll et al., 1978; García et al., 2021; Leney et al., 2018; Yamaji, 1980). Anthropogenic eutrophication, particularly nitrogen and phosphorus enrichment, intensifies bloom occurrence, with significant impacts on biogeochemical cycles and marine ecosystems (Sultana et al., 2022; Zhang et al., 2022). This phenomenon was observed near Menjangan Besar Island on September 19, 2023, where distinct red discolouration indicated an advanced bloom stage. These findings suggest that the bloom initiation likely occurred prior to September 12, 2023. However, spatiotemporal variation in the HAB development was observed at Bobby Beach and Legon Lele Beach, where green discolouration was recorded on September 19, 2023, indicating differences in bloom onset and progression across sites.

The level of toxicity is influenced by the specific type of microalgal present. Previous studies in KNP identified *Prorocentrum lima*, a toxic dinoflagellate linked to seagrasses (Widiarti et al., 2019). However, on September 19, 2023, HAB was dominated by *Trichodesmium erythraeum*, a bloom-forming cyanobacterium that disrupts biodiversity (Mohanty et al., 2010). Characterized by a 7–14-day life cycle, *Trichodesmium erythraeum* thrives under high nutrients, temperature, and low turbulence, releasing aerosolized cyanotoxins that cause respiratory issues, skin irritation, seafood contamination, and gastrointestinal illness. Additionally, it promotes secondary toxic blooms, compounding ecological and human health risks (Flores-Chavarria et al., 2023; Guo and Tester, 1994).

A HAB event is defined by an algal concentration exceeding 1,000,000 cells/L, which induces adverse ecological impacts (Sarkar, 2018). In this study, algae abundance was quantified using Stirling's formula (Stirling, 1999), with measurements conducted in triplicate, yielding a mean value of 18,496,000 cells/L. Accordingly, the observed event in KNP meets the threshold for HAB classification (Table 3).

Table 3. Calculation of microalgae abundance

Calculation of microalgae abundance	Results of the calculation of the abundance of *Trichodesmium erythraeum* (cells/L)
1st calculation	18,581,000
2nd calculation	18,258,000
3rd calculation	18,649,000
Average microalgae abundance	18,496,000

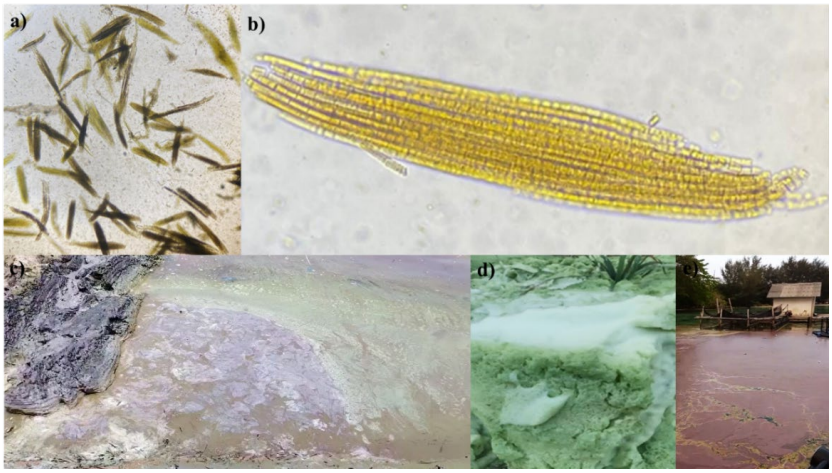

Fig.3. *Trichodesmium erythraeum* with magnification: a) 100x; b) 400x; c) harmful algal blooms (HABs) in surface water of Bobby Beach on September 19, 2023; d) green foam formed on Bobby Beach on September 19, 2023; e) algal blooming in surface water of Menjangan Besar Island on September 19, 2023.

3.2. Distribution values of Chl-a, nutrients, water quality, and current-hydrodynamics during algal blooming and post-HAB cleanup

The concentrations of Chl-a, nutrients, and water quality parameters during the HAB occurrence (September 19, 2023) and post-cleanup (September 22, 2023) are presented in Table 4. A clear relationship is observed between Chl-a and total suspended solids (TSS), where Chl-a primarily represents organic particulate matter, while TSS encompasses both organic and inorganic suspended particles larger than 2 μm, including sediment, algae, and bacteria (Yuan, 2021). This study confirms that phytoplankton, as indicated by Chl-a, contributes to TSS. However, TSS values consistently exceed Chl-a concentrations due to the presence of additional non-algae particles. During the HAB event in KNP, Chl-a concentrations reached exceptionally high levels of 198.557 μg/L at Bobby Beach and 569.679 μg/L at Menjangan Besar Island. TSS levels mirrored this trend, with values of 499.667 mg/L and 237 mg/L, respectively, demonstrating a direct correlation when Chl-a values are converted from μg/L to mg/L.

Table 4 reveals distinct Chl-a and TSS patterns at Menjangan Besar Island and Bobby Beach, indicating different wastewater sources. Menjangan Besar Island, influenced by Shrimp Pond A (west Karimunjawa Island), exhibits red seawater due to higher Chl-a concentrations, likely intensified by the bacterial decomposition of *Trichodesmium erythraeum*, which can temporarily sustain elevated Chl-a if algal cells remain intact (Satpathy et al., 2007). In contrast, Bobby Beach, affected by Shrimp Pond B (east Karimunjawa Island), shows higher TSS levels, driven by multiple factors, including suspended algal biomass, contributing to particulate matter. Moreover, extracellular polymeric substances (EPS) and mucilage secretion from *Trichodesmium erythraeum*, forming aggregates and high metabolic processes, release fine organic particles into the water column (Sudo, 1978). Furthermore, decomposition of particulate organic matter (POM) into dissolved organic matter (DOM), which interacts with metals in seawater, forming inorganic TSS (Du et al., 2022), and metal binding with sediments, clay, and silt, further increase TSS levels. These variations highlight the complex interactions between HAB activity, decomposition, and suspended solids, shaping water quality differences between the two sites.

The spatial distribution of Chl-a, TSS, and nutrients (ammonia, nitrate, phosphate, and silicate) during the HAB event on September 19, 2023, is illustrated in Fig. 4. Menjangan Besar Island exhibited higher Chl-a, lower TSS, and red seawater, contrasting with Bobby Beach, which remained in an earlier HAB phase. This pattern suggests advanced nitrogen cycle progression at Menjangan Besar Island, driven by bacterial decomposition, which transformed POM into DOM (Du et al., 2022), accumulating in water and sediment (Mickle, 1993). As a result, silicate, phosphate, and nitrate increased, while ammonia declined, indicating more active nitrification at Menjangan Besar Island than at Bobby Beach.

Nitrification is a crucial process in the marine nitrogen cycle, converting nitrogen into bioavailable forms essential for marine biota (Soratur et al., 2024). This biogeochemical cycle regulates nutrient availability, supports ecosystem productivity, and influences global nitrogen dynamics (Capone, 2008). Nitrification occurs in two stages (Arp and Stein, 2003), including ammonia (NH_3) oxidation to nitrite (NO_2^-) by nitrifying bacteria, requiring dissolved oxygen and providing energy for microbial metabolism. Moreover, nitrite (NO_2^-) oxidation to nitrate (NO_3^-), the primary nitrogen form assimilated by marine organisms (Beman et al., 2013). During the HAB event, Menjangan Besar Island

Table 4. Values of Chl-a, nutrients, water quality, and surface current hydrodynamics during algal blooming and after beach cleaning

Location and condition	Chl-a (μg/L)	TSS (mg/L)	Silicate (mg/L)	Phosphate (mg/L)	Ammonia (mg/L)	Nitrate (mg/L)	Temperature (°C)	DO (mg/L)	pH	Salinity (‰)	DIN : DIP	Currents (m/s)
Bobby Beach (AB)	198.557	499.667	0.005	0.453	0.584	46.029	28.747	6.244	7.926	33.487	102.842	0.145
Menjangan Besar Island (AB)	569.679	237.000	0.035	14.102	0.760	23.528	28.744	6.244	7.926	33.427	1.722	0.128
Shrimp Pond A (ABC)	20.651	392.667	0.019	0.009	0.456	0.224	28.494	6.448	8.027	34.675	76.921	0.133
MB1 (ABC)	1.807	28.333	0.003	0.031	0.146	0.238	28.492	6.448	8.027	34.688	12.402	0.120
MB2 (ABC)	1.587	19.667	0.005	0.011	0.036	0.163	28.492	6.448	8.027	34.688	18.062	0.120
MB3 (ABC)	1.484	24.667	0.005	0.042	0.602	0.143	28.491	6.448	8.027	34.688	17.724	0.120
BB1 (ABC)	12.043	180.000	0.007	0.011	0.511	0.190	28.496	6.448	8.027	34.701	63.410	0.130
BB2 (ABC)	2.671	17.667	0.004	0.062	0.036	0.156	28.496	6.448	8.027	34.701	3.115	0.130
BB3 (ABC)	3.141	18.000	0.004	0.007	0.002	0.109	28.496	6.448	8.027	34.702	16.634	0.130
LLB1 (ABC)	13.542	119.333	0.010	0.128	0.128	1.238	28.497	6.448	8.027	34.697	10.646	0.132
LLB2 (ABC)	2.559	49.667	0.003	0.007	0.018	0.136	28.497	6.448	8.027	34.697	23.253	0.132
LLB3 (ABC)	2.969	21.000	0.003	0.044	0.073	0.020	28.497	6.448	8.027	34.697	2.111	0.132

Note: AB (algal blooming); ABC (after beach cleaning); MB (Menjangan Besar); BB (Bobby Beach); LLB (Legon Lele beach); DIN (dissolved inorganic nitrogen); DIP (dissolved inorganic phosphorus)

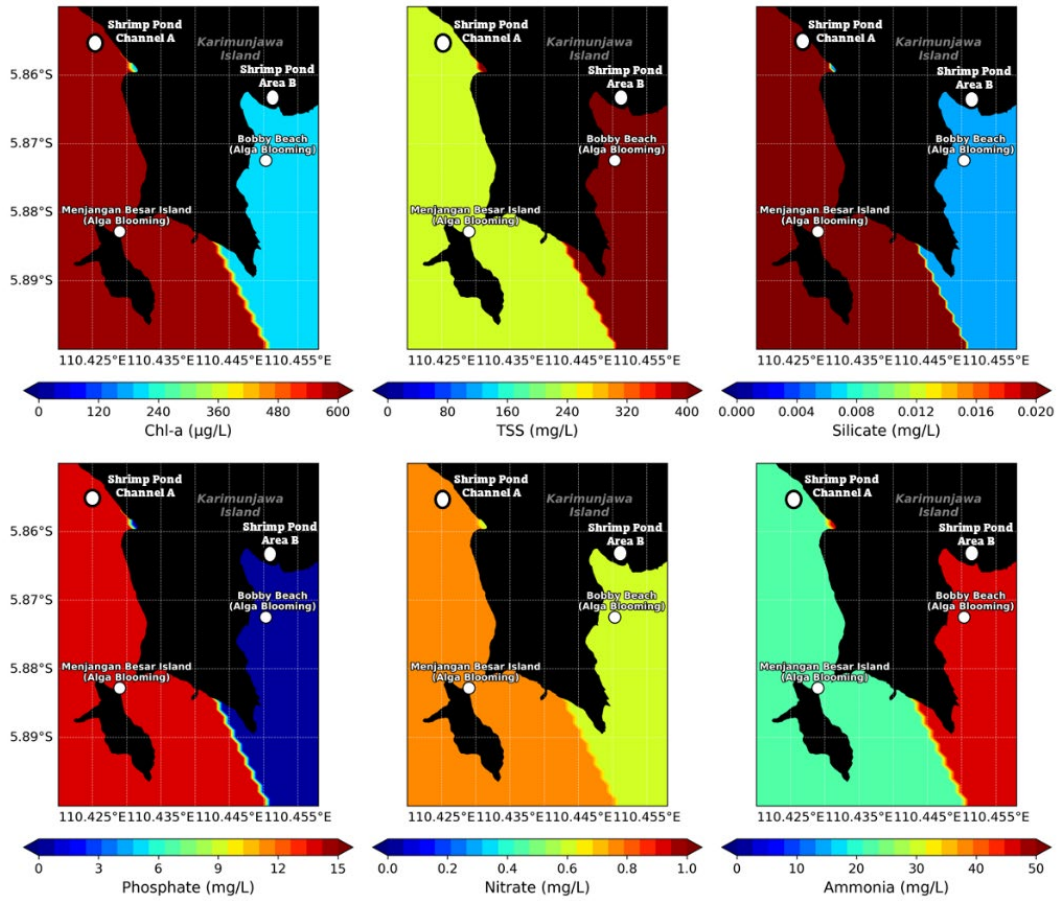

Fig.4. Distribution of Chl-a, TSS, silicate, phosphate, nitrate, and ammonia under HAB condition on September 19, 2023.

exhibited lower ammonia concentrations, suggesting active nitrification, as evidenced by higher nitrate levels compared to Bobby Beach. However, ammonia remained the dominant nutrient, indicating that eutrophication from shrimp pond wastewater, particularly from feed and fertilizer runoff, was the primary driver of elevated ammonia levels.

The DIN:DIP ratio indicates the balance between Dissolved Inorganic Nitrogen (DIN) and Dissolved Inorganic Phosphorus (DIP), reflecting nutrient balance and helping identify the limiting nutrient for phytoplankton growth (O'Neil et al., 2024). The Redfield ratio (16:1, N:P) represents optimal conditions (Knapp et al., 2012). In this study, DIN includes ammonia and nitrate, while DIP is based on phosphate (Table 4). DIN:DIP $>$ 16, found at Bobby Beach, indicates phosphorus limitation and potential for HABs. Conversely, DIN:DIP $<$ 16 at Menjangan Besar Island suggests nitrogen limitation, likely post-bloom. Moreover, the DIN:DIP ratio plays a role in regulating phytoplankton biomass. An imbalance in this ratio can favour the growth of certain phytoplankton species, potentially leading to the dominance of harmful algal species under nutrient-enriched conditions (Ma et al., 2025). These results underscore the DIN:DIP ratio as a governing factor of HAB dynamics.

The post-cleanup spatial conditions of HAB-affected areas (September 22, 2023) are depicted in Fig. 5. Sampling was conducted at Menjangan Besar Island, Bobby Beach, Legon Lele Beach, and a shrimp pond outlet, with shrimp pond A analysed for nutrient contributions. Of the 33 shrimp ponds in the study area, only the two closest (shrimp ponds A and B) were included. Following HAB cleanup via pumping, Chl-a, TSS, and nutrient concentrations significantly decreased compared to September 19, 2023.

Following post-HAB cleanup, Chl-a, TSS, and nutrient concentrations were significantly higher in the shrimp pond A outlet compared to other locations, confirming that shrimp pond effluent was the primary source of contamination. Although seawater from the shrimp pond A channel showed no visible discoloration on September 22, 2023, Chl-a (20.651 µg/L) and TSS (392.667 mg/L) remained elevated. Conversely, due to the greater distance from shrimp pond A, prior HAB removal, and seawater dilution, Chl-a and TSS levels at Menjangan Besar Island were substantially lower, at 1.807 µg/L and 28.333 mg/L, respectively.

On the east side, shrimp pond B discharge channel is located closest to Legon Lele Beach, followed by Bobby Beach. As a result, Chl-a concentrations were slightly higher at Legon Lele Beach (13.542 µg/L) compared to Bobby Beach (12.043 µg/L) due to its closer proximity to the nutrient source. However, TSS levels were higher at Bobby Beach (180 mg/L) than at Legon Lele Beach (119.333 mg/L) likely because of HAB conditions, further supported by the role of ocean currents in distributing TSS across the area. During the bloom, algae released mucus secretions and formed aggregates, contributing to increased suspended particles and the release of fine organic matter into the water column. Additionally, Chl-a and TSS values decreased further offshore due to dilution and hydrodynamic mixing (Liu et al., 2023).

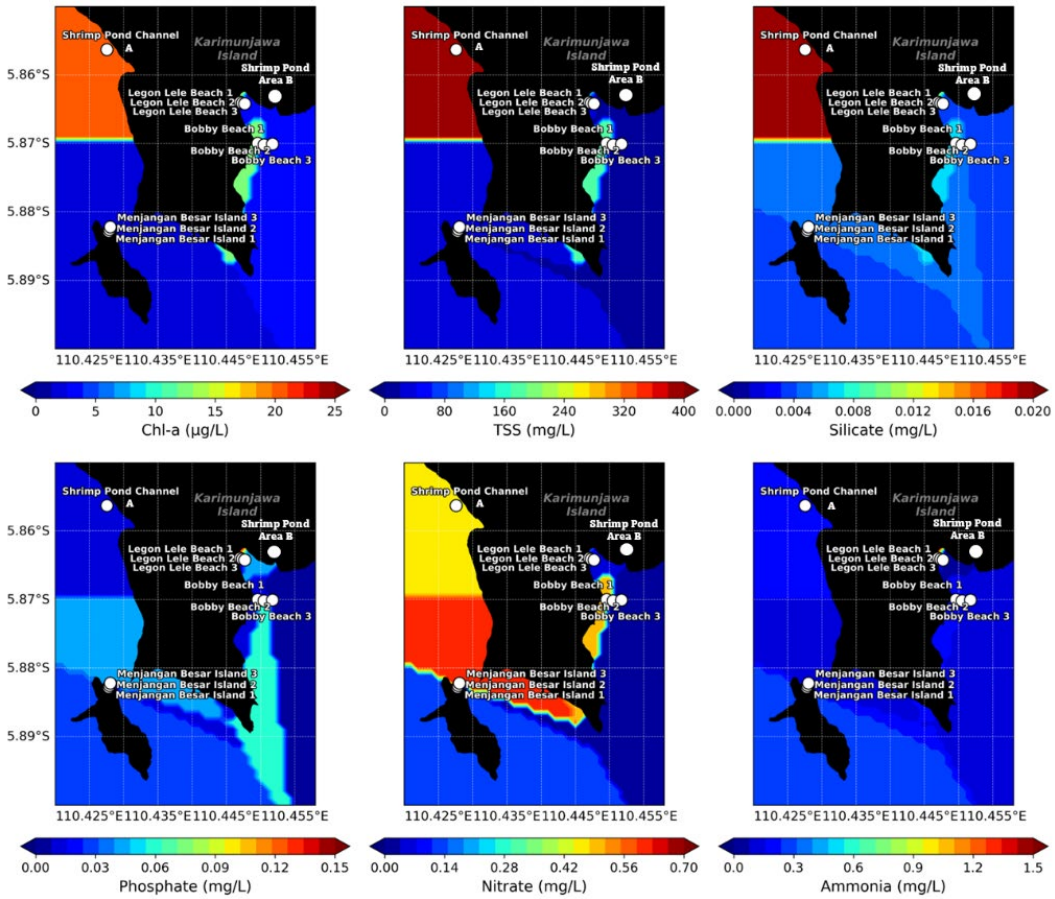

Fig.5. Distribution of Chl-a, TSS, silicate, phosphate; nitrate, and ammonia under after HAB clean-up condition on September 22, 2023.

The Chl-a and TSS patterns at Legon Lele Beach and Bobby Beach exhibit notable similarity, likely due to their proximity. However, a significant disparity is observed in ammonia concentrations, with Legon Lele Beach recording levels 10 times higher than Bobby Beach. This difference is attributed to the proximity of Legon Lele Beach to shrimp pond B wastewater discharge channel, which contains elevated ammonia levels. These findings indicate that the seawater in the area is heavily influenced by ammonia-rich effluent from shrimp pond B.

Hydrodynamic processes play a critical role in the formation and progression of HABs, influencing mixing, nutrient distribution, and water stratification (Yan et al., 2024). The results indicate that Chl-a, TSS, and nutrient concentrations generally decrease from the coastline seaward, primarily due to dilution by ocean currents, which facilitate water mass distribution and mixing. In this study, surface ocean currents, a key hydrodynamic factor, were analysed and are illustrated in Fig. 6.

Surface current patterns, derived from the numerical model, were classified into two conditions, including during HAB (Fig. 6a) and post-HAB cleanup (Fig. 6b). Hydrodynamic conditions significantly influence HAB development, with low current speeds (<0.24 m/s) promoting algal growth, enhancing energy metabolism and nutrient absorption (Song, 2023). In contrast, strong currents (>0.5 m/s) can disrupt algal metabolism, reduce oxidation levels, and cause cellular damage, limiting HAB persistence.

As shown in Fig. 6, surface current velocities ranging from 0.12 to 0.15 m/s were classified as low-current conditions during HAB and after clean-up

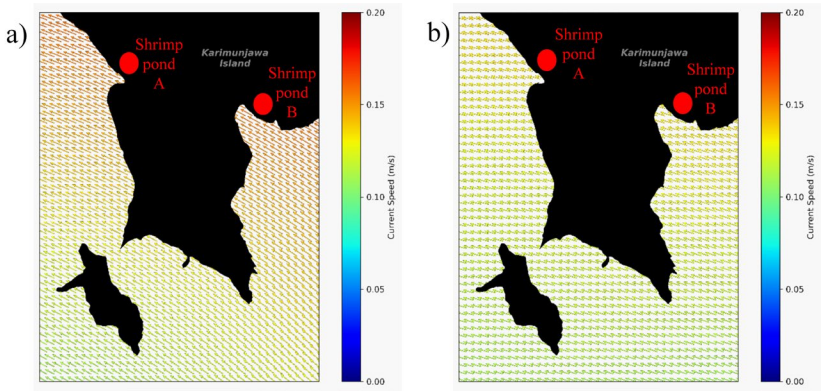

Fig.6. Sea surface current numerical model under: a) HAB condition at September 19, 2023; b) after HAB clean-up condition at September 22, 2023 (source: The Operational Mercator global ocean analysis and forecast, https://data.marine.copernicus.eu/product/GLOBAL_ANALYSISFORECAST_PHY_001_024/description).

conditions, which facilitated optimal algal growth and contributed to HAB formation. Low-current hydrodynamics contributes to HAB persistence, reducing mixing and keeping algae in surface layers by trapping nutrients and supporting prolonged bloom growth. Moreover, it enhances aggregation, increasing bloom intensity, and limits dispersal, leading to localized eutrophication. These factors collectively contribute to HAB persistence and expansion in low-energy aquatic environments.

The HAB event in September 2023 was influenced by the east monsoon, characterized by east-to-west winds, which played a significant role in hydrodynamic-driven nutrient transport. Surface currents facilitated the movement of effluent from shrimp pond A toward Menjangan Besar Island, leading to nutrient accumulation and HAB development. Similarly, discharges from pond B were transported toward Legon Lele Beach and Bobby Beach, further impacting coastal water quality and contributing to localized eutrophication.

3.3. Correlation between Chl-a, nutrients, water quality, and current hydrodynamics in KNP, Indonesia

PCA of Chl-a, nutrients, seawater quality, and current hydrodynamics (Table 5) quantifies linear relationships among variables, offering insights into key drivers of HAB formation and distribution. Results indicate a strong correlation between Chl-a and nutrient levels, with phosphate ($r = 0.952$), silicate ($r = 0.832$), ammonia ($r = 0.670$), and nitrate ($r = 0.653$), confirming that nutrient enrichment is a primary factor in HAB proliferation. These findings emphasize the role of eutrophication in sustaining algal blooms and highlight nutrient-driven mechanisms influencing bloom intensity and spatial distribution.

Additionally, Chl-a exhibits a positive correlation with sea surface temperature ($r = 0.877$) but negative correlations with salinity ($r = -0.892$), dissolved oxygen ($r = -0.880$), and pH ($r = -0.880$), indicating the influence of water quality parameters on HAB development. A moderate correlation was observed between Chl-a and TSS ($r = 0.448$), while currents showed a weak correlation ($r = 0.197$), suggesting a limited direct impact on HAB intensity but a potential role in HAB dispersion and spatial distribution. These findings highlight the critical role of nutrient enrichment and seawater quality in HAB formation, while hydrodynamic factors primarily influence their spread rather than initiation.

HAB formation is driven by sunlight, low currents, and nutrient dynamics. Nutrient levels peak before blooms and decline as microalgal metabolize them, with the DIN:DIP ratio playing a key role where nitrate triggers blooms, while phosphate limits growth (Sidabutar, 2016). Empirical evidence shows that high nitrate (DIN:DIP >16) at Bobby Beach coincided with active algal growth (green water), whereas phosphate dominance (DIN/DIP <16) at Menjangan Besar Island was linked to algal decomposition (red water). This supports findings by (Satpathy et al., 2007) concerning DIN:DIP that nitrogen initiates HABs (ammonia, $r = 0.525$; and nitrate, $r = 0.457$), while phosphate regulates their limiting factor ($r = -0.242$).

High ammonia levels and photosynthesis efficiency driven by solar radiation ($r = 0.877$) enhance algal growth, increasing bacterial activity and depleting dissolved oxygen. This process also lowers salinity and pH induced by algal ion uptake. Salinity is slightly reduced ($r = -0.892$), while CO_2 release during decomposition increases acidity ($r = -0.880$). Algae species exhibit varying salinity tolerances, including *Aureoumbra lagunensis* (Shi et al., 2024) and *Karenia mikimotoi* (Buskey et al., 1998) thriving in low-salinity waters, as well as *Halimeda* spp. tolerating hypersaline conditions. Additionally, green algae demonstrate a broad salinity range of 6.8–27.2 PSU (Taylor et al., 2001).

TSS showed a moderate correlation with Chl-a ($r = 0.448$) and a strong correlation with the DIN:DIP ratio ($r = 0.845$), reflecting the combined influence of living phytoplankton and dead organic matter. A high correlation with ammonia ($r = 0.745$) suggests significant biogeochemical interaction, beyond the presence of inorganic particles like sand and mud. This relationship is likely driven by organic waste and industrial effluents, where both TSS and ammonia contribute to eutrophication and HAB formation (Li et al., 2022). Additionally, a positive correlation with low-current

Table 5. Pearson correlation of Chl-a, TTS, nutrients, seawater quality, and currents.

Variables	Chl-a (µg/L)	TSS (mg/L)	Silicate (mg/L)	Phosphate (mg/L)	Nitrate (mg/L)	Ammonia (mg/L)	Temperature (°C)	DO (mg/L)	pH	Salinity (ppt)	DIN:DIP	Current (m/s)
Chl-a (µg/L)	1.000	0.448	0.832	0.952	0.653	0.670	0.877	-0.880	-0.880	-0.892	-0.001	0.197
TSS (mg/L)	0.448	1.000	0.443	0.218	0.657	0.745	0.670	-0.668	-0.666	-0.663	0.845	0.694
Silicate (mg/L)	0.832	0.443	1.000	0.878	0.630	0.307	0.560	-0.564	-0.563	-0.586	-0.011	0.043
Phosphate (mg/L)	0.952	0.218	0.878	1.000	0.552	0.414	0.692	-0.696	-0.696	-0.714	-0.242	-0.031
Nitrate (mg/L)	0.653	0.657	0.630	0.552	1.000	0.572	0.650	-0.655	-0.656	-0.665	0.457	0.159
Ammonia (mg/L)	0.670	0.745	0.307	0.414	0.572	1.000	0.943	-0.942	-0.941	-0.932	0.525	0.632
Temperature (°C)	0.877	0.670	0.560	0.692	0.650	0.943	1.000	-1.000	-1.000	-0.999	0.330	0.501
DO (mg/L)	-0.880	-0.668	-0.564	-0.696	-0.655	-0.942	-1.000	1.000	1.000	0.999	-0.328	-0.487
pH	-0.880	-0.666	-0.563	-0.696	-0.656	-0.941	-1.000	1.000	1.000	1.000	-0.326	-0.483
Salinity (ppt)	-0.892	-0.663	-0.586	-0.714	-0.665	-0.932	-0.999	0.999	1.000	1.000	-0.314	-0.466
DIN:DIP	-0.001	0.845	-0.011	-0.242	0.457	0.525	0.330	-0.328	-0.326	-0.314	1.000	0.609
Current (m/s)	0.197	0.694	0.043	-0.031	0.159	0.632	0.501	-0.487	-0.483	-0.466	0.609	1.000

hydrodynamics (r = 0.694) supports the role of water retention in facilitating algal accumulation. These findings highlight the importance of suspended particles in nutrient transport and their broader impact on water quality and ecosystem health.

PCA was conducted to simplify complex multidimensional relationships and extract meaningful patterns within the dataset (Patel et al., 2024). This technique reduces the number of variables while preserving essential information by generating uncorrelated principal components (PCs), which are linear combinations of the original variables (Lever et al., 2017). The primary objective of PCA is to maximize variance capture, allowing for optimal data interpretation while minimizing information loss. By facilitating pattern recognition and dimensionality reduction, PCA enhances the efficiency and clarity of statistical analysis, making it a valuable tool for identifying key environmental drivers in the dataset.

PCA of HABs in KNP (Fig. 7) illustrates the relationships among nutrients, water quality, and hydrodynamic factors. Red arrows represent environmental variables, with similar directions indicating positive correlations, and longer arrows reflecting stronger influences on PCs. Rightward vectors, contributing predominantly to PC1, are closely associated with bloom conditions. PCA results align with Pearson correlations, showing strong associations between Chl-a and both phosphate and silicate, while ammonia shows the weakest nutrient correlation. DO, pH, and salinity are negatively correlated with Chl-a, indicating that HABs favour low-oxygen, low-salinity, and acidic conditions. TSS is strongly linked to Chl-a, reflecting increased algal biomass. Hydrodynamic influence appears at low currents, reinforcing nutrient enrichment as the primary driver of HABs. Additionally, DIN:DIP maintains a positive correlation with HABs, supporting its role in both bloom development and post-bloom conditions.

PCA results indicate that Bobby Beach, representing the active bloom phase, is strongly driven by nutrient enrichment, particularly nitrate and ammonia. In contrast, Menjangan Besar Island, associated with the bloom decomposition phase, is more influenced by silicate and phosphate, with lower overall nutrient input. Green-marked cleanup sites (Shrimp Pond and MB1–MB3) show improved water quality, while blue and purple sites (BB1–BB3 and LLB1–LLB3) reflect further nutrient reduction, confirming cleanup effectiveness. The clear distinction between green, blue and purple sites implies varying effluent sources influencing spatial differences in water quality.

The correlation analysis provides insights into HAB formation (Fig. 8), characterized by elevated Chl-a concentrations driven by high nutrient availability, particularly POM from shrimp pond waste. Microbial activity converts DOM into bioavailable nutrients, releasing ammonia, phosphate, and silicate. Through nitrification, ammonia is oxidized to nitrite and subsequently to nitrate, fuelling phytoplankton growth illustrated in Fig. 8(C1). Sufficient sunlight and low-current hydrodynamics further enhance HAB outbreaks.

HAB depletes DO through algal respiration and microbial decomposition of dead algae, leading to hypoxic or anoxic conditions that may trigger toxin production, threatening marine ecosystems depicted in Fig. 8(C2). HAB also impact water quality, causing slightly lower salinity due to ion uptake during algal growth and reduced pH as decomposing algae release CO_2, forming carbonic acid and increasing water acidity shown in Fig. 8(C3). Additionally, TSS levels rise due to increased algal biomass (organic TSS) and inorganic TSS from DOM binding with metals and sediments.

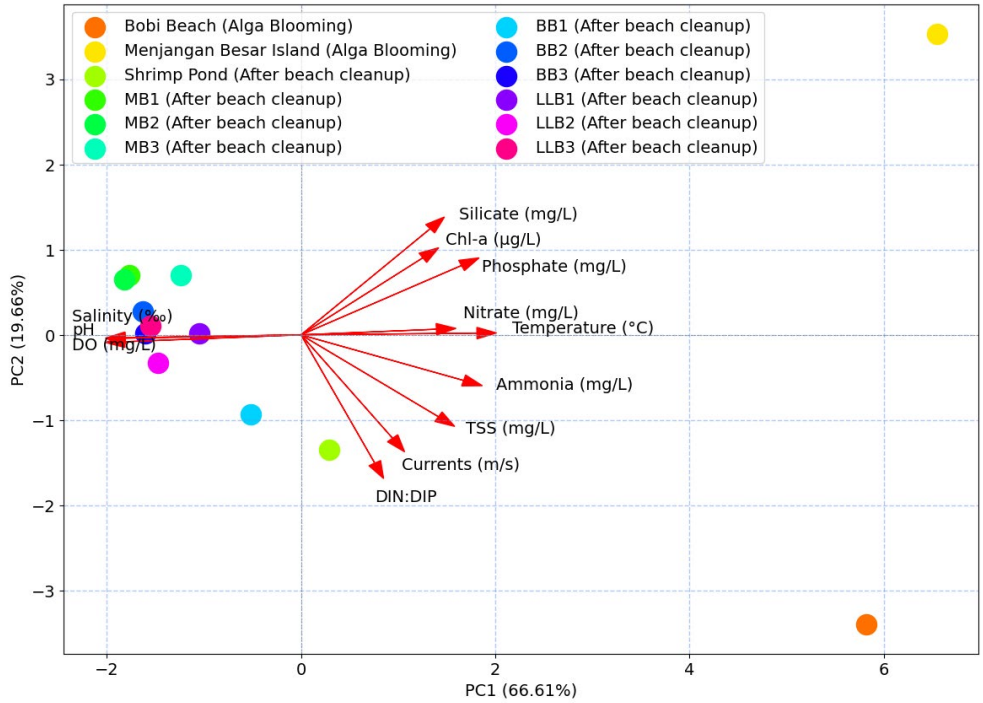

Fig.7. PCA analysis of Chl-a to nutrients, water quality, and hydrodynamic factors.

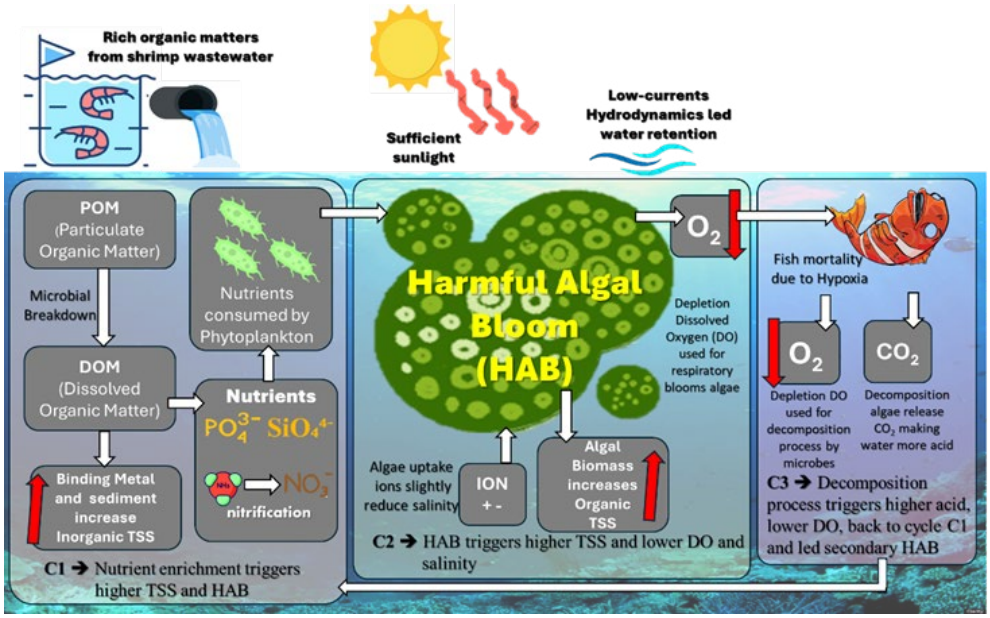

Fig.8. Mechanism of HABs in KNP.

4. Conclusions

The HAB outbreak in Karimunjawa National Park (KNP) on September 19, 2023, occurred under optimal bloom conditions, primarily driven by elevated nutrient inputs linked to Vannamei shrimp harvest cycles. These anthropogenic inputs were further intensified by intense sunlight during the dry season peak and the presence of low-current hydrodynamics, which collectively created a favourable environment for algal proliferation. The bloom event exemplifies a disturbance in the coastal biogeochemical cycle. It initiates with nutrient enrichment (chemical phase), transitions into rapid microalgal growth (biological phase), and proceeds to decomposition (geochemical phase). This terminal stage can result in hypoxic conditions, increasing the risk of secondary HABs that may exhibit heightened severity due to toxin production and further oxygen depletion.

Acknowledgements

This research was conducted under the Research, Development, and Application (RPP) Program of the Institution of Research and Community Service (LPPM), Diponegoro University, with funding support from the APBN of Universitas Diponegoro (2024) and Visiting Lecturer Program of World Class University, Faculty of Fisheries and Marine Science, Diponegoro University (2025). The authors express their sincere gratitude to all funding institutions and contributors, whose support was instrumental in the successful completion of this study. The research was carried out in accordance with institutional guidelines, as stipulated in the Activity Assignment Letter No. 569-02/UN7.D2/PP/VII/2024 issued by LPPM, Universitas Diponegoro.

Conflict of Interest

The authors declare no conflicts of interest.

References

American Public Health Association (APHA). 2005. American Water Works Association, & Water Environment Federation. Standard Methods for the Examination of Water and Wastewater (21st ed.). Washington, DC: APHA.

Apostolopoulos D., Nikolakopoulos K.G., Boumpoulis V. et al. 2020. GIS based analysis and accuracy assessment of low-resolution satellite imagery for coastline monitoring. Proceedings Volume 11534, Earth Resources and Environmental Remote Sensing/GIS Applications XI: 115340B. DOI: 10.1117/12.2573440

Arp D.J., Stein L.Y. 2003. Metabolism of Inorganic N Compounds by Ammonia-Oxidizing Bacteria. Critical Reviews in Biochemistry and Molecular Biology 38(6): 471–495. DOI: 10.1080/10409230390267446

Beman J.M., Leilei Shih J., Popp B.N. 2013. Nitrite oxidation in the upper water column and oxygen minimum zone of the eastern tropical North Pacific Ocean. ISME Journal 7(11): 2192–2205. DOI: 10.1038/ismej.2013.96

Boyd C.E., Prather E.E., Parks R.W. 1975. Sudden Mortality of a Massive Phytoplankton Bloom. Source: Weed Science 23(1): 61–97. URL: https://www.jstor.org/stable/4042459?seq=1&cid=pdf-

Buskey E.J., Wysor B., Hyatt C. 1998. The role of hypersalinity in the persistence of the Texas 'brown tide' in the Laguna Madre. In Journal of Plankton Research 20(8): 1553–1565. URL: https://academic.oup.com/plankt/article/20/8/1553/1483528

Capone D.G. 2008. The marine nitrogen cycle. Microbe 3(4): 186–192. DOI: 10.1128/microbe.3.186.1

Chan L., Li Y., Stenstrom M.K. 2008. Protocol Evaluation of the Total Suspended Solids and Suspended Sediment Concentration Methods: Solid Recovery Efficiency and Application for Stormwater Analysis. Water Environment Research 80(9): 796–805. DOI: 10.2175/106143008x296497

Coll R.M., Edwards M.R., Haaksma C. 1978. Some properties of allophycocyanin from a thermophilic blue-green alga. Biophysical Chemistry 8: 369–376. DOI: 10.1016/0301-4622(78)80018-0

Ding X., Liu J., Zhang H. et al. 2022. Phytoplankton Community Patterns in the Northeastern South China Sea: Implications of Intensified Kuroshio Intrusion During the 2015/16 El Niño. Journal of Geophysical Research: Oceans 127(2): e2021JC017998. DOI: 10.1029/2021JC017998

Doering P.H., Chamberlain R.H., Haunert K.M. 2006. Chlorophyll-a and its use as an indicator of eutrophication in the Caloosahatchee Estuary, Florida. Lessons Learned from Transferring Science to Watershed Management 69: 51–72.

Du Y.X., An S.L., He H. et al. 2022. Production and transformation of organic matter driven by algal blooms in a shallow lake: Role of sediments. Water Research 219(1): 118560. DOI: 10.1016/j.watres.2022.118560

Endean R., Monks S.A., Griffith J.K. et al. 1993. Apparent relationships between toxins elaborated by the Cyanobacterium Trichodesmium Erythraeum and those present in the flesh of the Narrow-barred Spanish Mackerel Scomberomorus Commersoni. Toxicon 31(9): 1155–1165. DOI: 10.1016/0041-0101(93)90131-2

Flores-Chavarria A.M., Rodríguez-Jaramillo C., Band-Schmidt C.J. et al. 2023. Effect of dissolved metabolites of the dinoflagellate Gymnodinium catenatum (Graham, 1943) on the white shrimp *Litopenaeus vannamei* (Boone, 1931): A histological study. Heliyon 9(6): e17018. DOI: 10.1016/j.heliyon.2023.e17018

Fraga M., Churro C., Leão-Martins J. et al. 2025. Cyanotoxins on the move - Freshwater origins with marine consequences: A systematic review of global changes and emerging trends. Marine Pollution Bulletin 216: 118017. DOI: 10.1016/j.marpolbul.2025.118017

Frankenberg N., Mukougawa K., Kohchi T. et al. 2001. Functional Genomic Analysis of the HY2 Family of Ferredoxin-Dependent Bilin Reductases from Oxygenic Photosynthetic Organisms. The Plant Cell 13(4): 965–978. DOI: 10.1105/tpc.13.4.965

García A.B., Longo E., Bermejo R. 2021. The application of a phycocyanin extract obtained from Arthrospira platensis as a blue natural colorant in beverages. Journal of Applied Phycology 33(5): 3059–3070. DOI: 10.1007/s10811-021-02522-z

Guiry M.D., Guiry G.M. 2023. AlgaeBase. World-wide electronic publication, National University of Ireland, Galway (taxonomic information republished from AlgaeBase with permission of M.D. Guiry). *Trichodesmium erythraeum Ehrenberg ex Gomont, 1892*. through: World Register of Marine Species. URL: https://marinespecies.org/aphia.php?p=taxdetails&id=660919 (Accessed 2023-09-2)

Guo C., Tester P.A. 1994. Toxic effect of the bloom-forming Trichodesmium sp. (cyanophyta) to the copepod Acartia tonsa. Natural Toxins 2(4): 222–227. DOI: 10.1002/nt.2620020411

Harvey E.T., Walve J., Andersson A. et al. 2019. The effect of optical properties on secchi depth and implications for eutrophication management. Frontiers in Marine Science 5: 496. DOI: 10.3389/fmars.2018.00496

Johan F., Jafri M.Z., Lim H.S. et al. 2014. Laboratory measurement: Chlorophyll-a concentration measurement with acetone method using spectrophotometer. In: 2014 IEEE International Conference on Industrial Engineering and Engineering Management, pp. 744–748. DOI: 10.1109/IEEM.2014.7058737

Knapp A.N., Dekaezemacker J., Bonnet S. et al. 2012. Sensitivity of *Trichodesmium erythraeum* and *Crocosphaera watsonii* abundance and N_2 fixation rates to varying NO_3^- and PO_4^{3-} concentrations in batch cultures. Aquatic Microbial Ecology 66(3): 223–236. DOI: 10.3354/ame01577

Leney A.C., Tschanz A., Heck A.J.R. 2018. Connecting color with assembly in the fluorescent B-phycoerythrin protein complex. FEBS Journal 285(1): 178–187. DOI: 10.1111/febs.14331

Lessard E.J., Swift E. 1986. Short Communication Dinoflagellates from the North Atlantic classified as phototrophic or heterotrophic by epifluorescence microscopy. Journal of Plankton Research 8(6). DOI: 10.1093/plankt/8.6.1209

Lever J., Krzywinski M., Altman N. 2017. Points of Significance: Principal component analysis. Nature Methods 14(7): 641–642. DOI: 10.1038/nmeth.4346

Li M., Zhang H., Sun H. et al. 2022. Effect of phosphate and ammonium concentrations, total suspended solids and alkalinity on lignin-induced struvite precipitation. Scientific Reports 12(1): 2901. DOI: 10.1038/s41598-022-06930-0

Liu J., Qiu Z., Feng J. et al. 2023. Monitoring Total Suspended Solids and Chlorophyll-a Concentrations in Turbid Waters: A Case Study of the Pearl River Estuary and Coast Using Machine Learning. Remote Sensing 15(23): 5559. DOI: 10.3390/rs15235559

Liu X.S. 2019. A probabilistic explanation of Pearson's correlation. Teaching Statistics 41(3): 115–117. DOI: 10.1111/test.12204

Ma W., Feng J., Zhang J. et al. 2025. Different responses of phytoplankton taxa to water N and P inputs in a freshwater wetland: A mesocosm study. Marine Pollution Bulletin 216: 117895. DOI: 10.1016/j.marpolbul.2025.117895

Mickle A.M. 1993. Pollution filtration by plants in wetland-littoral zones. Proceedings of the Academy of Natural Sciences of Philadelphia 144: 282–290. URL: https://www.jstor.org/stable/4065012

Mohanty A.K., Satpathy K.K., Sahu G. et al. 2010. Bloom of *Trichodesmium erythraeum* (Ehr.) and its impact on water quality and plankton community structure in the coastal waters of southeast coast of India. Indian Journal of Marine Science 39(3): 323–333. URL: https://nopr.niscpr.res.in/handle/123456789/10669

Morabito S., Silvestro S., Faggio C. 2018. How the marine biotoxins affect human health. Natural Product Research 32(6): 621–631. DOI: 10.1080/14786419.2017.1329734

Morris A.W., Riley J.P. 1963. Determination of nitrate in sea. Analytica Chewca Acta 29: 272–279. DOI: 10.1016/S0003-2670(00)88614-6

Mullin J.B., Riley J.P. 1955. The colorimetric determination of silicate with sl'ecial reference to sea and natural waters. Analytica chimica acta 12: 162–176. DOI: 10.1016/S0003-2670(00)87825-3

Murphy J., Rilley J.P. 1962. A modified single solution method for the determination of phosphate in natural waters. Analytica chimica acta 27: 31–36. DOI: 10.1016/S0003-2670(00)88444-5

O'Neil J.M., Heil C.A., Glibert P.M. et al. 2024. Plankton Community Changes and Nutrient Dynamics Associated with Blooms of the Pelagic Cyanobacterium *Trichodesmium* in the Gulf of Mexico and the Great Barrier Reef. Water (Switzerland) 16(12): 1663. DOI: 10.3390/w16121663

Paerl H.W., Valdes-Weaver L.M., Joyner A.R. et al. 2007. Phytoplankton indicators of ecological change in the eutrophying Pamlico sound system, North Carolina. Ecological Applications 17(sp5): S88-S101. DOI: 10.1890/05-0840.1

Parsons T.R., Maita Y., Lalli C.M. 1984. A Manual of Chemical & Biological Methods for Seawater Analysis-Pergamon Press. A. Wheaton & Co. Ltd. Exeter.

Patel K., Tiwary G.J., Pandey K.K. et al. 2024. An unsupervised machine learning algorithm: PCA (Principal Component Analysis) comprehensive review. International Research Journal of Modernization in Engineering Technology and Science 6(2): 1303–1314. DOI: 10.56726/irjmets49457

Polak M., Heiser W.J., de Rooij M. 2009. Two types of single-peaked data: Correspondence analysis as an alternative to principal component analysis. Computational Statistics and Data Analysis 53(8): 3117–3128. DOI: 10.1016/j.csda.2008.09.010

Purnomo A., Mufti P., Takarina N. et al. 2022. Environmental Impact of the Intensive System of Vannamei Shrimp (*Litopenaeus vannamei*) Farming on the Karimunjawa-Jepara-Muria Biosphere Reserve, Indonesia. International

Journal on Advanced Science, Engineering and Information Technology 12: 873. DOI: 10.1016/j.csda.2008.09.010

Qijun L. 2010. Reviews of influences from hydrodynamic conditions on algae. Soil and Environmental Sciences 19(7): 1732–1738.

Sarkar S.K. 2018. Marine algal bloom: Characteristics, causes and climate change impacts. Springer Nature Singapore. DOI: 10.1007/978-981-10-8261-0

Satpathy K.K., Mohanty A.K., Sahu G. et al. 2007. On the occurrence of *Trichodesmium erythraeum* (Ehr.) bloom in the coastal waters of Kalpakkam, east coast of India. Indian Journal of Science and Technology 1(2): 1–9. DOI: 10.17485/ijst/2007/v1i1/29204

Satya E.D., Sabdono A., Wijayanti D.P. et al. 2023. Mapping coral cover using Sentinel-2A in Karimunjawa, Indonesia. Biodiversitas 24(2): 827–836. DOI: 10.13057/biodiv/d240219

Shi X., Zou Y., Zhang Y. et al. 2024. Salinity decline promotes growth and harmful blooms of a toxic alga by diverting carbon flow. Global Change Biology 30(6): e17348. DOI: 10.1111/gcb.17348

Sidabutar T. 2016. Mass Mortality of Fish in Lampung Bay, Indonesia. Omni Akuatika 12(2): 17–25. DOI: 10.20884/1.oa.2016.12.1.27

Sidqi J., Agroqua F.D.J., Fidari J.S. et al. 2022. The design model of intensive Vaname Shrimp Ponds for eco-green aquaculture development in the area of Probolinggo, East Java, Indonesia. Agroqua 20(1): 24–39.

Song Y. 2023. Hydrodynamic impacts on algal blooms in reservoirs and bloom mitigation using reservoir operation strategies: A review. Journal of Hydrology 620: 129375. DOI: 10.1016/j.jhydrol.2023.129375

Soratur A., Venmathi Maran B.A., Kamarudin A.S. et al. 2024. Microbial Diversity and Nitrogen Cycling in Peat and Marine Soils: A Review. Microbiology Research 15(2): 806–822. DOI: 10.3390/microbiolres15020052

Stirling H.P. 1999. Chemical and Biological Methods of Water Analysis for Aquaculturists. Pisces. University of Stirling Institute of Aquaculture.

Sudo R. 1978. Some ecological observation on the decomposition of periphytic algae and aquatic plants (Vol. 12). Pergamon Press.

Sultana S., Awal S., Shaika N.A. et al. 2022. Cyanobacterial blooms in earthen aquaculture ponds and their impact on fisheries and human health in Bangladesh. Aquaculture Research 53(15): 5129–5141. DOI: 10.1111/are.16011

Taylor R., Fletcher R.L., Raven J.A. 2001. Preliminary Studies on the Growth of Selected “Green Tide” Algae in Laboratory Culture: Effects of Irradiance, Temperature, Salinity and Nutrients on Growth Rate. Botanica Marina 44(4): 327–336. DOI: 10.1515/BOT.2001.042

Veldhuis M.J.W., Kraay G.W. 2000. Flow cytometry analysis of phytoplankton 121. Scientia Marina 64(2): 121–134. DOI: 10.3989/scimar.2000.64n2121

Wang L., Wang X., Jin X. et al. 2017. Analysis of algae growth mechanism and water bloom prediction under the effect of multi-affecting factor. Saudi Journal of Biological Sciences 24(3): 556–562. DOI: 10.1016/j.sjbs.2017.01.026

Weber M., De Beer D., Lott C. et al. 2012. Mechanisms of damage to corals exposed to sedimentation. Proceedings of the National Academy of Sciences of the United States of America 109(24): E1558-E1567. DOI: 10.1073/pnas.1100715109

Widiarti R., Zamani N.P., Bengen D.G. et al. 2019. The dinoflagellate causing ciguatera fish poisoning, Prorocentrum lima, in Karimunjawa island waters-Central Java. IOP Conference Series: Earth and Environmental Science 325(1): 012014. DOI: 10.1088/1755-1315/325/1/012014

Wijaya A., Pramono S.E., Melati I.S. et al. 2021. Toward the Community-based Sustainable Marine Tourism: Identifying the Impact of Tourism Development in Karimunjawa Island. International Journal of Academic Research in Business and Social Sciences 11(5): 275–288. DOI: 10.6007/IJARBSS/v11-i5/9924

Wijayanti D.P., Indrayanti E., Nuryadi H. et al. 2018. DNA barcode of Acropora hyacinthus of Karimunjawa Archipelago. IOP Conference Series: Earth and Environmental Science 139(1): 012017. DOI: 10.1088/1755-1315/139/1/012017

Yamaji I. 1980. Illustrations of the marine plankton of Japan. Hoikusha no genshoku zukan 45: 537.

Yan Z., Kamanmalek S., Alamdari N. et al. 2024. Comprehensive Insights into Harmful Algal Blooms: A Review of Chemical, Physical, Biological, and Climatological Influencers with Predictive Modeling Approaches. Journal of Environmental Engineering 150(4). DOI: 10.1061/JOEEDU.EEENG-7549

Yuan L.L. 2021. Continental-scale effects of phytoplankton and non-phytoplankton turbidity on macrophyte occurrence in shallow lakes. Aquatic Sciences 83(1): 14. DOI: 10.1007/s00027-020-00769-1

Yuliana E., Boer M., Fahrudin A. et al. 2017. Biodiversity of reef fishes in marine protected area of Karimunjawa National Park. Jurnal Ilmu Dan Teknologi Kelautan Tropis 9(1): 29–43. DOI: 10.29244/jitkt.v9i1.17915 (In Bahasa)

Zadorojny C., Saxton S. 1973. Spectrophotometric Determination of Ammonia. Finger Source: Journal (Water Pollution Control Federation) 45(5): 905–912. URL: https://www.jstor.org/stable/i25037822

Zhang W., Liu J., Xiao Y. et al. 2022. The Impact of Cyanobacteria Blooms on the Aquatic Environment and Human Health. Toxins 14(10): 658. DOI: 10.3390/toxins14100658